

**Project:** WT-285

**Title:** Modeling the dual-slope behavior of in-quad EL-FEXT in twisted pair quad cables

**Source:** Rob F.M. van den Brink  
TNO, the Netherlands  
[Rob.vandenBrink@tno.nl](mailto:Rob.vandenBrink@tno.nl)

**Date:** July 25-28, 2016, Berlin

**Distribution:** Metallic Transmission Group

### Abstract:

This contribution contains a paper on the cause of the dual slope effect in quad cables. It is based on an advanced modeling approach, and is currently under review by IEEE for possible publication. It is provided to support our proposal (bbf2016.687) for a simplified EL-FEXT model covering this dual slope effect. A slides presentation about this topic can be found in our contribution bbf2016.685.

## 1 Background

One of the reasons why FEXT levels are getting so pronounced is that above a certain frequency the EL-FEXT increases with 40 dB/decade instead of the usual 20 dB/decade. This effect was raised in our ITU contribution of February 2012 [2] and called the “dual slope effect”. Since then the existence of that “dual slope” effect was confirmed by many others and observed in various different cables [3,4,5,6,7,8,9,10,11,12,13,14], and many other contributions thereafter.

So far the phenomenon was not well understood and resulted in a number of conjecture explanations [15] in both the Broadband Forum as in ITU-T. As a result it was not clear how to model that and how the far end crosstalk changes with the loop length.

Recent studies at TNO have learned that the dual slope effect is caused by a combination of two independent phenomena's: a first order and a second order crosstalk effect. Both effects can exist without the other, are completely independent from each other, and each of them differently with the cable length.

- The origin of the first order effect is well known [16, 17] and random in nature. Its magnitude in the EL-FEXT scales proportionally with the *root* of the cable length (in a statistical sense).
- The origin of the second order effect is deterministic in nature (assuming that the cable geometry is deterministic as well) and scales proportionally with the length.

The sum of both has a dual slope appearance and the break frequency between both slopes depends on the magnitude of each crosstalk effect.

This contribution is the covering letter of a scientific paper about this topic, which is currently under review by IEEE for possible publication [1]. It is for information only and is to support our proposal in bbf2016.687 on a simplified EL-FEXT model covering this dual slope effect. The slides of a presentation that TNO has recently presented (July 29<sup>th</sup>, 2016) at the UFBB-Seminar in den Haag (the Netherlands) about this topic gives more guidance on the approach in this paper. These have been attached to contribution bbf2016.685.

## 2 Summary

This contribution is provided for information but with the goal of improving the collection of cable modelling techniques brought together in TR-285.

## 3 References

- [1] Rob F.M. van den Brink, “*Modelling the dual-slope behavior of EL-FEXT in twisted-pair quad cables*” Submitted in January 2016 to IEEE for possible publication, revised on May 2016 and still under review at the time of writing.
- [2] TNO (Rob van den Brink, Bas van den Heuvel), “*Dual slope behavior of EL-FEXT*”, contribution 2012-02-4A-038 to ITU-T-SG15/Q4, Feb 2012.
- [3] Brink, “*Far-End crosstalk in twisted pair cabling: measurements and modeling*”, TNO Contribution 11RV-022, ITU-T SG15/Q4, Nov 2011.
- [4] Eriksson, Berg, Lu; “*Equal Length FEXT measurements on PE05 cable*”, Ericsson Contribution 11RV-054R1, ITU-T SG15/Q4, Richmond, November 2011.
- [5] Huawei, “*Equal-Length FEXT Measurements on PE05 Cable*”, Huawei Contribution COM 15 - C 1864, ITU-T SG15/Q4, November 2011.
- [6] Bruyssel, Maes “*Dual slope behaviour of EL-FEXT*”, ALU Contribution 2012-06-4A-033, ITU-T SG15/Q4, May 2012.
- [7] Humphrey, “*On dual slope FEXT observations*”, BT Contribution 2012-05-4A-021, ITU-T SG15/Q4, May 2012.
- [8] Humphrey, Morsman, “*FEXT cable measurements*”, BT Contribution 2012-05-4A-025, ITU-T SG15/Q4, May 2012.
- [9] Muggenthaler, Tudziers; “*EL-FEXT Analysis*”, DT Contribution 2012-06-4A-041, ITU-T SG15/Q4, May 2012.
- [10] Bongard, “*Dual slope ELFEXT behaviour on Swiss cables*”, Swisscom contribution 2013-01-Q4-042, ITU-T SG15/Q4, Feb 2013.
- [11] Kozarev, Strobel, Leimer, Muggenthaler, “*Modeling of Twisted-Pair Quad Cables for MIMO Applications*” Lantiq/DT Contribution bbf2014.467, BroadbandForum, june 2014 (updated from bbf2014.377 and bbf2014.117).
- [12] Heuvel, Trommelen, Brink, “*G.fast: Preliminary analysis of the transfer characteristics of the 104 m KPN Access cable*”, TNO Contribution 2013-03-Q4-026, March 2013.
- [13] Heuvel, “*G.vector: High in-quad crosstalk coupling in older cables*”, TNO Contribution 2015-10-Q4-024, ITU-T SG15/Q4, Oct 2015.
- [14] Heuvel, “*G.vector: High crosstalk coupling in older cables – Measurements on GPLK01*”, TNO Contribution 2015-11-Q4-028, ITU-T SG15/Q4, Dec 2015.
- [15] Schneider, Kerpez, Starr, Sorbara “*Transfer Functions, Input Impedance and Noise Models for the Loop End*”, Cosigned contribution bbf2014.066.00, BroadbandForum, March 2014.
- [16] *Transmission systems for communications*. Bell Telephone Labs, 1971, 4th edition.
- [17] ETSI TR 101 830-2, Spectral Management on metallic access networks, Part 2: Technical methods for performance evaluations, revision V1.2.1, 2008.

# Modeling the dual-slope behavior of in-quad EL-FEXT in twisted pair quad cables

Rob F.M. van den Brink

**Abstract**—It is well known that the ratio between received crosstalk and received signal in telephony cabling increases with the frequency until both levels become about equal. Transmission systems like VDSL and G.fast are designed to cope with that. But the awareness that the increase of EL-FEXT (equal level - far end cross talk) becomes much stronger above a certain frequency (increases with 40 dB instead of 20 dB per decade) was raised only recently in ITU and BBF standardization bodies for G.fast. This second order phenomenon became known under the name "dual slope" effect, was initially not well understood, and resulted in a number of conjectured explanations. This paper demonstrates that this second order effect in far end crosstalk between opposite wire pairs in the same quad is deterministic in nature. It is caused by the interaction of the twist in a quad with wires and its metallic surroundings (e.g. shield). The twist of these quads reduces this second order crosstalk effect significantly, but what remains causes a slope of 40 dB/decade. This paper shows via a model that this second order effect scales linearly with the cable length. It quantifies how sensitive this effect is to cable design parameters like twist length and capacitance to shield. In addition, an extension is proposed to a commonly used simplified system model for describing the far end cross talk as a function of the frequency and cable length.

**Index Terms**—Twisted pair cables, far-end crosstalk, EL-FEXT, transmission line theory, cable modeling, digital subscriber line (DSL)

## 1 INTRODUCTION

DIGITAL subscriber line (DSL) modems, aimed for the next generation broadband via copper [1], are designed to transmit their signals through multi-pair telephony cables under noisy stress conditions. This noise originates via crosstalk from other DSL systems using other wire pairs in the same cable. Most of this crosstalk can be eliminated by proper vectoring techniques [2], a technique that has become common within DSL systems, and required by G.fast [3] and VDSL [4] standards (VDSL=Very high speed DSL). But these crosstalk levels can even exceed the levels of the DSL signals beyond some break-frequency at given cable length [5], [6]. This puts strong demands on vector engines to handle these high crosstalk levels as well. G.fast can transmit signals up to 106 MHz (and in future up to 212 MHz) and recent versions of VDSL up to 35 MHz.

*Rob F.M. van den Brink is with TNO, Den Haag, The Netherlands, e-mail: Rob.vandenBrink@tno.nl.*

*This work has been submitted to the IEEE for possible publication. Copyright may be transferred without notice, after which this version may no longer be accessible.*

Using these frequencies required the development of more advanced models for twisted pair cables up to hundreds of MHz [7], [8], [9].

Legacy models on crosstalk [10], [11] assume that the ratio between far-end crosstalk and signals transmitted via the direct channel (the equal level - far end crosstalk or just EL-FEXT) increases in frequency with a slope of 20 dB/decade and increases in length with the square-root of the cable length. But more recent measurements focused on higher frequencies revealed a dual-slope behavior of the EL-FEXT [5], [6], [12] showing a second order crosstalk effect of 40 dB/decade as well. This second order effect has a significant impact on the usability of higher frequency bands by DSL systems and their vectoring engines. This is because the effect doubles the slope of the EL-FEXT above some break frequency, becomes dominant thereafter and break frequencies as low as 2 MHz have been observed as well.

This behavior was raised [5], [12] in ITU-T SG15/Q4, which is the standardization body for VDSL and G.fast, and was soon confirmed by others [13], [14], [15], [16], [17], [18], [19]. It was clearly visible between wire pairs in the same quad within several multi-quad cables, and observed to be cable-type and quad dependent, but the effect was not so visible or sometimes invisible in the available cable measurements between different quads.

Initially the cause was not well-understood, and this resulted in a number of conjectured explanations for the dual slope effect, as summarized in [20]:sect5.2. One conjecture [20] is the normal, expected behavior of coupled transmission lines. Another conjecture [20] is that it is the "upward" ramp of a resonance which takes place beyond 106 MHz. This resonance is the result of parasitic mutual inductance and mutual capacitance. A third conjecture [20] is that it is the result of propagation through the various "phantom" or alternate paths that can couple two loops.

The phenomenological dependence on coupling length was suggested in [15], [18] on the basis of available measurements. Although [18] also related the dual slope effect to the twist of the wires and the shield, that paper did not quantify the effect via modeling. The more recent TR-285 [21], [22] from Broadband Forum is illustrative for the state of the art on cable models, and refers to the dual slope effect as just "experimental observations". It models (in A.2.3.4) the EL-FEXT with just two straight lines (one for each slope) and models the length dependency of both the first and second order effect equally, and proportionally with  $\sqrt{L}$ .

It also describes a full multi-port cable model, and phrases (in section B.1.5.4) the opposite: that length dependency of the in-quad crosstalk is “in general” proportionally with the length  $L$ . In spite of the capabilities of that advanced model, TR-285 [21] does not detail on the cause of both slopes and on the fact that they both scale differently with the loop length. As a result, a good understanding on how the characteristics of this second order effect relates to various cable characteristic is currently lacking.

The present paper shows via modeling that the cause of the second order crosstalk effect of in-quad FEXT is different and independent from the well known first order effect and will also scale differently with the cable length. The presence of both effects gives the EL-FEXT its dual slope effect. This second order effect is caused by deterministic variations in the geometry of the wiring with respect to their shield, and is also present in the absence of random perturbations (causing the first order effect).

As opposed to a brute force modeling approach in [23], [21], [24], the present paper is restricted to the modeling of a single quad (4 wires with a common twist) with respect to a shield. The aim is to gain understanding on the physical mechanism causing the observed behavior. A full description on how multiple quads in the same cable will interact is kept out-of scope of this paper. This simplifies complex matters significantly and allows for exploring the most striking dependencies of the dual slope effect in various dimensions. Section 2 starts with a brief summary of measurements to show how this second order effect is visible in EL-FEXT between opposite wire pairs in the same quad. The existence of this crosstalk effect between different quads of a multi-quad cable is a bit inconclusive from available measurements and that question is considered as out-of-scope of this paper. Section 3 elaborates on a full eight-port model of four wires in a quad to study the impact of twisting four wires in the vicinity of a shield to gain understanding. Section 4 to 6 provide novel material, by building further on cascaded models and explores the dependency of the effect in various dimensions. Section 4 shows how reliable this approach is, section 5 analyses how sensitive the second order slope is to various design parameters of a cable and section 6 analyse how the second order effect scales with the cable length. The eight-port model is quite reliable but often too complicated for simple system calculations on modem performance. Therefore we propose in section 7 an extension to a commonly used simplified model for EL-FEXT to cover the first and second slope and their length-dependencies as well. A preliminary version of this paper is meanwhile contributed to ITU-T SG15/Q4 as [25] to assist the relevant standardization groups with further understanding on the dual slope effect.

## 2 MEASUREMENT RESULTS

To illustrate the dual slope effect, we selected a characterization [6] of a multi-pair telephony cable, 378m in length and wound on a drum, where the wires are organized in groups of four (30 twisted quads in total, similar to figure 4) and where the cable has a common shield. Measurements were performed directly on the individual wires (using the shield as common) by means of an 8-port network

analyzer, without balanced transformers and with full 8-port correction of systematic measurement errors [6], [26].

The measured  $s$ -parameters represent all possible direct transmission, reflection and crosstalk values of four individual wires with respect to a common ground (an 8-port has 64 of these values). But DSL modems are using these wires in pairs, and are connected to them via balanced transformers. Therefore the differential mode transmission and crosstalk through or between these wires pair were calculated from these 64 numbers. The results are shown in figure 1 to 3.

### 2.1 Observations on crosstalk

Figure 1 shows two curves, the upper curve “TRAN” representing the measured balanced transmission in a wire pair of a quad, and the lower curve “FEXT” representing the far end crosstalk to that wire pair from the other pair in the quad. The FEXT increases with the frequency, and beyond about 50 MHz the crosstalk levels are even higher than the direct transmission levels.

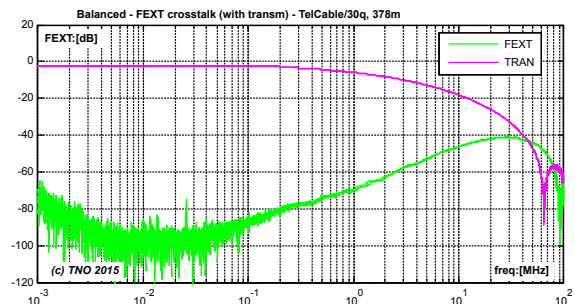


Fig. 1. Transmission and FEXT, measured in both directions of a 378m multi quad telephony cable.

Figure 2 shows a curve “ELFEXT” which is the ratio between the levels of received crosstalk and signal at the other side of the cable and called the “equal level FEXT”. It is evaluated as the (magnitude of the) ratio between measured “FEXT and “TRAN” from figure 1. Two additional asymptotic lines, labeled as “slope 1” (of 20 dB/decade) and “slope 2” (of 40 dB/decade), are drawn to highlight the dual slope effect of this EL-FEXT curve.

The asymptotic lines cross each other near 2 MHz, but that break frequency is cable, quad and length dependent. So in this example the second slope becomes dominant above about 2 MHz and affects almost the full VDSL band. This dependency is clearly visible in measurements on different cable types as reported in [5]. Values ranging from 1 MHz to 15 MHz have been observed. Above 60 MHz, the EL-FEXT “resonates” around 0 dB. This is typical behavior as observed in many cables, is well-predictable by our model in section 3 (and shown in figure 7), but not simply related to a single quantifier. It is not really related to noise and/or randomness and could be referred to as “a complex composition of various higher order effects”.

Figure 3 shows two curves, each of them representing the measured phase of the EL-FEXT from a first wire pair to the second one in the same quad, and from the second to the first pair. This phase has a random appearance up to about 100 kHz, where the first order slope dominates. This

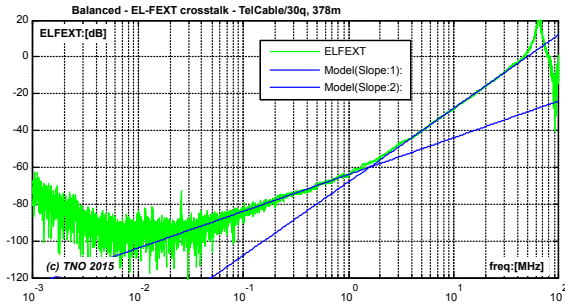


Fig. 2. The dual slope behavior of the magnitude of the EL-FEXT (20 and 40 dB/decade).

is indicative for a random origin of the first order behavior of the EL-FEXT. Above about 2 MHz, the phase converges to constant (deterministic) values up to about 60 MHz; the band where the second order slope dominates. The lack of randomness where the second order effect dominates is indicative for a more deterministic origin of it, and makes it plausible that the second order effect is an independent (deterministic) effect of EL-FEXT, independent from and coexisting with the (random) first order effect. Therefore the randomness gradually disappears when the frequency increases from about 100 kHz to 2 MHz until deterministic values dominate the phase. Moreover, the pairs of forward crosstalk coupling functions in the quad converge to opposite sign, a behavior that is also typical within quads where the dual-slope effect is clearly visible. Above 60 MHz the phase gives the impression to become random again. But this is more due to rapid phase variations by the above mentioned “higher order effects” and they can also be reasonably described by the model in section 3 (as shown in figure 8).

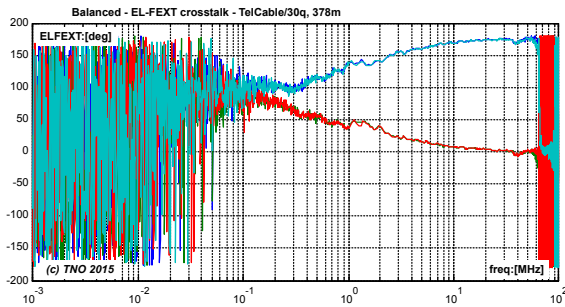


Fig. 3. The phases of both forward EL-FEXT transfers in a quad converge to opposite signs between 1 and 60 MHz.

**2.2 Description of first and second order effects**

The cause of the first order slope (20 dB/decade) is well known [10], [11]. If the centers of four wires in a quad are perfectly positioned at the corners of a square, and balanced signals are using opposite wires as a pair, then all crosstalk to the other wire pair in the same quad will be zero due to perfect symmetry. But the smallest deviation from that perfection will already result in some residual crosstalk. This causes the well-known first order crosstalk

effect, since real cables will always have small imperfections in the symmetry of their quads, which are also randomly distributed along the cable length. Twisting does not really help against this crosstalk within the same quad; it helps minimizing the crosstalk between wire pairs from other quads.

But there is also another crosstalk effect, as will be discussed in the rest of this paper via simulation. If the geometry in the quad is of perfect shape, but the quad is in the vicinity of a shield (or conductive surroundings like other quads) then the electrical symmetry within the quad is disturbed since each wire may have a slightly different capacitive coupling to that shield. This can be minimized by twisting the full quad, and after many twists each wire has on average the same capacitance to shield. The tighter the quad is twisted the better this works and the less disturbance the shield will have on the electrical symmetry. But there will always be a residue, causing a small amount of extra crosstalk, and our model can quantify that this deterministic effect causes the second order slope (40 dB/decade).

**3 SIMULATION APPROACH**

The wire pairs in a multi quad cable are organized in groups of four wires, as shown in figure 4, and surrounded by a common shield. Each pair (1-2) or (3-4) of opposite wires is being used in a balanced mode. When the geometry of such a quad is a perfect square, and when the quad is far away from the shield and other quads, then the symmetry will cause that the crosstalk from one balanced pair (1-2) to the other balance pair (3-4) in the same quad is zero. But this is not the case in practice, for instance when the quad is in the vicinity of a shield. Then each wire has an additional capacitance to that shield (and to other quads) as well, as shown in the circuit equivalent of figure 4.

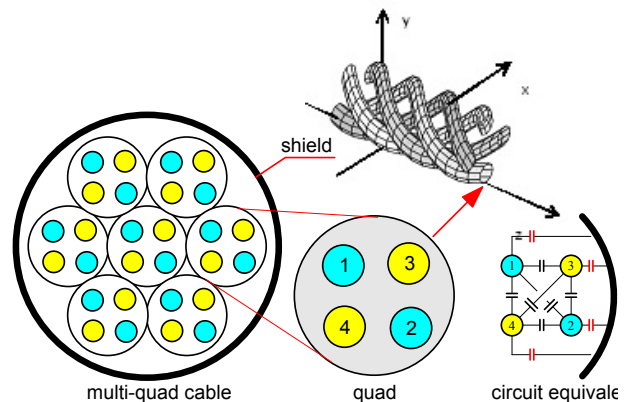


Fig. 4. A multi-quad cable is organized in groups of four wires positioned in a square, and each quad is twisted many times over its full length. Opposite wires (1-2) and (3-4), are used for (balanced) transmission, and each wire has a capacitance to all the other wires and to the common shield. The drawing of the helical structure was copied from a picture in [21].

This capacitance is not equal for each wire and thus deteriorates the overall symmetry of the quad. This is one of the reasons why quads are twisted so that each wire approaches the shield as often as the other three over each

twist length. This makes all wire capacities to shield equal on average, restores the balance on average and reduces the overall crosstalk significantly.

To model this twisting effect, we consider the cable as a long cascade of very short cable sections of four wire structures. If the length of each section is short enough (compared to the twist length) then they can be assumed as piece-wise uniform over its length. Each section may have different uniformity but this will be repetitive if the wires are regularly twisted. One can obtain the transfer functions of interest by treating each uniform section with four wires as an 8-port (using the shield as common), by cascading them all over the full cable length as 8-ports, and by extracting from that cascade the overall balanced transfers of the wire pairs.

### 3.1 Modeling uniform cable sections

A complete modeling of each uniform cable section can be obtained via the well-known multi-conductor transmission line equations [27]:ch3, [8], [24], [23], [21]. When  $z$  denotes the longitudinal position in this cable structure, then the vectors of voltages  $\mathbf{U}$  and currents  $\mathbf{I}$  are at each position  $z$  given by the matrix collection:

$$\begin{aligned} \frac{\partial}{\partial z} \mathbf{U}(z) &= -\mathbf{Z}_s \cdot \mathbf{I}(z) \\ \frac{\partial}{\partial z} \mathbf{I}(z) &= -\mathbf{Y}_p \cdot \mathbf{U}(z) \end{aligned} \quad (1)$$

In these expressions,  $\mathbf{Z}_s$  is the series impedance matrix per unit length and  $\mathbf{Y}_p$  the shunt admittance matrix. If we split them into their real and imaginary parts we may phrase them as  $\mathbf{Z}_s = \mathbf{R}_s + j\omega\mathbf{L}_s$  and  $\mathbf{Y}_p = \mathbf{G}_p + j\omega\mathbf{C}_p$ . Note that all these matrices are in principle non-zero and frequency dependent. This description can be thought of as an alternating cascade of infinite thin (inductive) series networks and (capacitive) shunt networks, as depicted in figure 5.

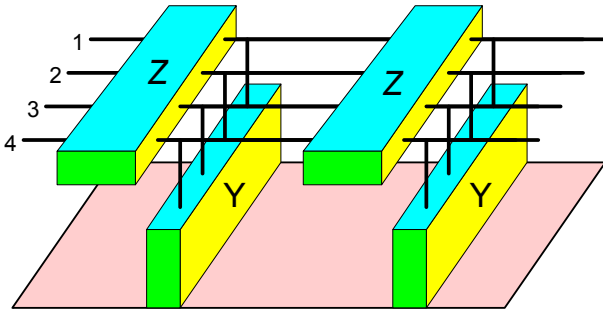


Fig. 5. An alternating cascade of infinite thin networks can represent a uniform cable.

The series impedance matrix  $\mathbf{Z}_s$  is dominantly inductive in nature representing the series inductance (per unit length) of individual wires and their mutual magnetic coupling. By adding series resistors we can account for the cable loss. The shunt admittance matrix  $\mathbf{Y}_p$  is dominantly capacitive in nature representing all capacitive coupling (per unit length) between the wires and the shield.

Figure 6 shows a circuit diagram with lumped elements of this concept if a uniform 4-wire structure is surrounded by a shield and is perfectly loss-free. This concept can easily be generalized for more wires. If losses are involved then

the circuit diagram can be extended with (low) resistors in series with the inductors and by adding a small loss-angle to the capacitors. In principle, none of these lumped elements are zero nor frequency in-dependent.

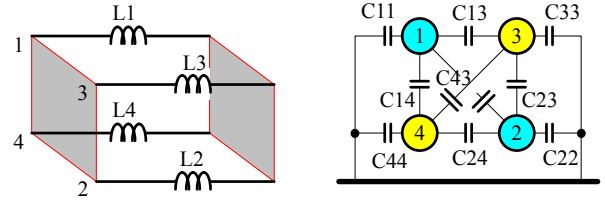


Fig. 6. The Z-matrix is inductive in nature and the Y-matrix is capacitive in nature.

Cable modeling is essentially the finding of parametric expressions to evaluate the matrices  $\mathbf{Z}_s$  and  $\mathbf{Y}_p$  as function of the frequency. Once these matrices are modeled, a full multi-port cable model of a uniform section is simply the evaluation of multi-port s-parameters from a pair  $\{\mathbf{Z}_s, \mathbf{Y}_p\}$  via common calculation methods [27], [24], [21]. Similarly, a cascade of uniform sections is modeled via additional cascade calculations with multi-port s-parameters [27]. These modeled s-parameters are to be the same as those that have been measured directly on the cable, otherwise the model is inadequate. From this point the evaluation of cable properties such as EL-FEXT are the same as those used after measurements.

The aim of this paper is not to make the best possible cable model that handles all cable details very well, but to make the simplest model that is adequate enough to raise understanding on the cause of the dual slope effect. One such simplification is assuming that all dielectric losses are zero, that both  $\mathbf{C}_p$  and  $\mathbf{L}_s$  are frequency-independent and that all cable loss is caused by series resistance. To model however cable loss sufficiently fair over a wide frequency interval, each series resistance should be modeled with a strong frequency dependency to address additional losses caused by the skin effect in each wire.

Effort on two-port cable modeling up to hundreds of MHz [7], [8], [9] has learned that this simplification is not entirely true but that the capacitance is rather constant over a wide frequency interval, the inductance converges roughly to a constant value above a few hundreds of kHz, and that dielectric losses are small compared to resistive losses. Extracted matrix values for  $\mathbf{C}_p$  and  $\mathbf{L}_s$  from multi-port cable measurements [6] show a similar behavior over a sufficient wide frequency interval. The error we make by using the above mentioned simplification is irrelevant for raising the aimed understanding, since the resulting multi-port cable model can still offer a sufficiently good match between model and measurements (as will be shown in figure 7).

### 3.2 Modeling matrices C, L and R of uniform sections

To model  $\mathbf{Y}_p$  from this example structure we therefore assume  $\mathbf{G}_p = 0$  and assume  $\mathbf{C}_p$  to be frequency-independent. In other words, we assume only ideal lumped capacitors between the wires and/or shield, where  $C_{rk} = C_{kr}$  denotes the lumped capacitance per unit length between wire  $r$  and

$k$ , and  $C_{kk}$  between wire  $k$  and the common shield. By transforming this lumped circuit description into its Y-parameter representation, we obtain the desired (symmetric)  $\mathbf{Y}_p$  for a 4-wire structure:

$$\mathbf{Y}_p = j\omega \cdot \mathbf{C}_p = j\omega \cdot \begin{bmatrix} \sum C_1 & -C_{12} & -C_{13} & -C_{14} \\ -C_{21} & \sum C_2 & -C_{23} & -C_{24} \\ -C_{31} & -C_{32} & \sum C_3 & -C_{34} \\ -C_{41} & -C_{42} & -C_{43} & \sum C_4 \end{bmatrix} \quad (2)$$

Where  $\sum C_r = C_{r1} + C_{r2} + C_{r3} + C_{r4} = C_{1r} + C_{2r} + C_{3r} + C_{4r}$ .

To model the imaginary part of  $\mathbf{Z}_s$  from our example structure we assume  $\mathbf{L}_s$  to be frequency-independent (the measurements reported in [6] show that this is a fair approximation), and its real part by a simple frequency-dependency for  $\mathbf{R}_s$ . In other words we assume for  $\mathbf{L}_s$  only ideal lumped inductors that are all magnetically coupled, and for  $\mathbf{R}_s$  resistors in series with these inductors. Similarly to  $\mathbf{C}_p$  we can model  $\mathbf{L}_s$  independently by assuming lumped inductance and coupling values. However this approach can easily result in cable models predicting properties that are physically impossible. Therefore it is often more convenient to evaluate  $\mathbf{L}_s$  via a detour.

Lets therefore assume another (hypothetical) wiring structure where all copper is exactly the same as the real one but where all insulation around that copper is assumed to be fully absent. In other words: as if all conductors are suddenly floating in vacuum. Such a hypothetical wiring structure has different properties and the inductance and capacitance matrices will change accordingly from  $\{\mathbf{L}_s, \mathbf{C}_p\}$  to  $\{\mathbf{L}_{s0}, \mathbf{C}_{p0}\}$ . What we gain from that approach is (a) that now  $\mathbf{L}_{s0}$  can easily be derived from  $\mathbf{C}_{p0}$ , (b) that  $\mathbf{L}_s$  can easily be derived from  $\mathbf{L}_{s0}$  and that (c)  $\mathbf{C}_{p0}$  is relatively simple to estimate from the values of  $\mathbf{C}_p$ .

Lets clarify that step by step. The first step (a) is possible since the free-space matrix relation  $\mathbf{L}_{s0} \times \mathbf{C}_{p0} = \mathbb{I}/c_0^2$  holds for this hypothetical structure. See [27]:eq3.37, [8]:eq4. In this expression, matrix  $\mathbb{I}$  refers to the identity matrix and constant  $c_0 = 3 \cdot 10^8$  m/s refers to the speed of light in vacuum. Step (b) is possible since  $\mathbf{L}_s$  and  $\mathbf{L}_{s0}$  have equal values since the magnetic properties of the actual and hypothetical structure are the same (only the dielectric properties have changed). Step (c) is a bit more complicated. If all insulation has vanished then all lumped capacitances reduce in value by a factor roughly equal to the dielectric constant(s) of the used insulation material. Typically a value somewhere between about 2.0 and 4.0 for real telephony cables. Estimating realistic values for these scaling factors is less critical then directly estimating realistic values for the mutual inductances in  $\mathbf{L}_s$ , and this makes the use of above detour less error-prone and therefore more convenient.

In conclusion, when  $\epsilon_{rk}$  represents the scaling for lumped capacitance  $C_{rk}$  to  $C_{rk0} = C_{rk}/\epsilon_{rk}$ , then we can create  $\mathbf{L}_s$  via expression (3). And since  $\epsilon_{rk} = \epsilon_{kr}$  and  $C_{rk} = C_{kr}$ , only three independent  $\epsilon$  values are to be estimated for a perfect symmetrical quad structure to extract  $\mathbf{L}_s$  from  $\mathbf{C}_p$ .

To complete the modeling of  $\mathbf{Z}_s$  with its real part, we also assume  $\mathbf{R}_s$  as the result of 4 lumped resistors, in series with the four lumped inductors in  $\mathbf{L}_s$ . This simplifies  $\mathbf{R}_s$  into a diagonal matrix since the dielectric is assumed to act as perfect insulator. These resistors are to be frequency-

$$\mathbf{L}_s = \frac{1}{c_0^2} \cdot \begin{bmatrix} \sum CE_1 & -C_{12}/\epsilon_{12} & -C_{13}/\epsilon_{13} & -C_{14}/\epsilon_{14} \\ -C_{21}/\epsilon_{21} & \sum CE_2 & -C_{23}/\epsilon_{23} & -C_{24}/\epsilon_{24} \\ -C_{31}/\epsilon_{31} & -C_{32}/\epsilon_{32} & \sum CE_3 & -C_{34}/\epsilon_{34} \\ -C_{41}/\epsilon_{41} & -C_{42}/\epsilon_{42} & -C_{43}/\epsilon_{43} & \sum CE_4 \end{bmatrix}^{-1} \quad (3)$$

Where  $\sum CE_r = C_{r1}/\epsilon_{r1} + C_{r2}/\epsilon_{r2} + C_{r3}/\epsilon_{r3} + C_{r4}/\epsilon_{r4}$

dependent to account for the skin-effect in the wires, and when modeled such a curve in a pure mathematical manner then a simple truncated series expansion in  $\sqrt{\omega}$  can model this dependency quite well. If each wire  $r$  adds an equal series resistance to each inductor, then this diagonal matrix  $\mathbf{R}_s$  becomes:

$$\mathbf{R}_s = \left( R_{s0} + \sqrt{\frac{\omega}{\omega_0}} \cdot R_{s1} + \frac{\omega}{\omega_0} \cdot R_{s2} + \dots \right) \cdot \begin{bmatrix} 1 & 0 & 0 & 0 \\ 0 & 1 & 0 & 0 \\ 0 & 0 & 1 & 0 \\ 0 & 0 & 0 & 1 \end{bmatrix} \quad (4)$$

Where  $R_{s0}, R_{s1}, \dots$  are all constants and  $\omega_0 = 2\pi \cdot 1MHz$

The nominal values in table 1 are chosen to offer a good match between the cable measurements in the figures 1, 2 and 3, and what the model predicts. This match will be demonstrated in figure 7 and 8. These nominal values are found in an iterative manner, starting from estimated values for  $C$  and  $\epsilon$ . These estimations were taken from [6], where both the cable measurements as well as the extracted values for  $\mathbf{C}$  and  $\mathbf{L}$  were reported for this particular cable. These first estimates gave already a fair match and could be manually improved by tuning the values and inspecting the match between the measurements and what the model predicts in terms of s-parameters.

Nominal values for  $\{R_{s0}, R_{s1}, R_{s2}, \dots\}$  were also found in an iterative manner. A starting value for  $R_{s0}$  was obtained via low-frequency measurements of series resistance and the other values were initially assumed to be zero. They were also improved via manual iteration, by comparing the measured cable loss with the loss predicted via these numbers. A fair match could be achieved (see figure 7 and 8) with only the first three terms of the series expansion of  $\mathbf{R}_s$  as non-zero. The rest of the polynomial expansion was truncated.

TABLE 1  
Nominal parameter values, to simulate a section

$C_{11} \approx C_{22} \approx C_{33} \approx C_{44}$	$C_c$	10	pF/m
$C_{31} \approx C_{42} \approx C_{32} \approx C_{41}$	$C_p$	22	pF/m
$C_{21} \approx C_{43}$	$C_q$	9.5	pF/m
$\epsilon_{11} \approx \epsilon_{22} \approx \epsilon_{33} \approx \epsilon_{44}$	$\epsilon_c$	3.3	
$\epsilon_{13} \approx \epsilon_{42} \approx \epsilon_{32} \approx \epsilon_{41}$	$\epsilon_p$	2.5	
$\epsilon_{21} \approx \epsilon_{43}$	$\epsilon_q$	3.1	
$R_{s0}$	$R_{s0}$	0.0863	$\Omega/m$
$R_{s1}$	$R_{s1}$	0.130	$\Omega/m$
$R_{s2}$	$R_{s2}$	0.018	$\Omega/m$

With only 9 nominal values per unit length, a full multi-port parameter description of this symmetric and uniform line can be evaluated from the matrices  $\mathbf{Z}_s$  and  $\mathbf{Y}_p$ , as outlined in section 3.1.

In our case, we transformed them all into single wire s-parameters for the full cable and from that into mixed mode parameters for the balanced wire pairs.

### 3.3 Modeling the twist in the quad

The full cable however is not uniform because the twist in the wires causes the distance between each wire and the shield to vary with the  $z$  position in that cable. As a result the capacity from wire to shield varies regularly from a minimum to a maximum value, and back. We have approximated this over a full twist length by cascading  $n$  uniform but slightly different sections, where  $n$  varied between 4 and 64. The four capacitance values from the wires to the shield vary gradually as well with the position of each section while all other values in table 1 are kept at their nominal value. The theoretical capacitance between two flat metallic plates is roughly inversely proportional with the distance  $d$ . This property is used here as well to estimate how the capacitance between wire and shield varies with the distance. The twist varies this distance in a harmonic manner over a full twist length  $\Delta L$ , and therefore this variance in segment  $k$  has been modeled as:

$$\begin{aligned} C_{11} &= C_c / (1 + \Delta_c \cdot \sin(2\pi \cdot k/n \cdot \Delta L)) \\ C_{22} &= C_c / (1 - \Delta_c \cdot \sin(2\pi \cdot k/n \cdot \Delta L)) \\ C_{33} &= C_c / (1 + \Delta_c \cdot \cos(2\pi \cdot k/n \cdot \Delta L)) \\ C_{44} &= C_c / (1 - \Delta_c \cdot \cos(2\pi \cdot k/n \cdot \Delta L)) \end{aligned} \quad (5)$$

Where  $\Delta_c$  is a chosen "shield unbalance" factor,  $\Delta L$  the twist length,  $n$  the number of steps per twist,  $k$  an integer index of the section, and  $C_c$  a nominal value taken from table 1. The full cable can subsequently be approximated by repeating this cascade as often as needed for creating the full cable length (over 16000 sections in our example cable). This is a brute force approach, but allows us to analyze various cable properties.

TABLE 2  
Parameter values used to simulate the twisting

Sections per twist	"n"	$n$	16
Twist length	"dL"	$\Delta L$	37cm
Shield unbalance	"dc"	$\Delta_c$	0.55

## 4 SIMULATION ACCURACY

### 4.1 Match between model and data

The modeling approach of the previous chapter in combination with the nominal values from table 1 and 2 offers a close prediction of the measured cable properties of our example cable. Figure 7 illustrates how close the magnitudes of measured and modeled transmission and far end crosstalk can be with above mentioned values. It shows two measured and two modeled curves, one representing the transmission through a wire pair and the other representing the far end cross talk between two wire pair of the same quad. Both show a good match up to high frequencies and even the dip in the transmission around 65 MHz is well predicted by the model. The match between the curves in figure 7 become weaker for the highest frequencies, and is most pronounced by the deviation of the measured and modeled dip around 90 MHz. This small deviation is not a surprise since all values of the inductance and capacitance matrices have been modeled as frequency in-dependent (to keep the model as simple as possible), while multi-port

measurements on this cable have shown [6] that both vary a bit with the frequency. Since all geometric imperfections of the quad were ignored, except for the twist and for a shield, these dips are apparently caused by the interaction between twist and shield.

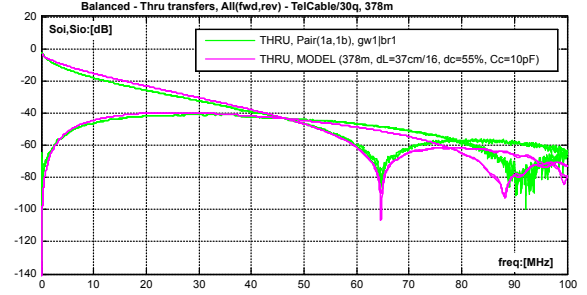


Fig. 7. Match of transmission and FEXT magnitudes, between model and measurement.

Figure 8 shows the match between measured and modeled phase of the two EL-FEXT curves of a quad in forward direction. Our model predicts a phase of 0 and 180 degrees between the two EL-FEXT curves in forward direction and this holds for the frequencies above about 2 MHz (from where the second order effect dominates the crosstalk) until about 60 MHz (from where the EL-FEXT has approached its asymptotic value of 0 dB).

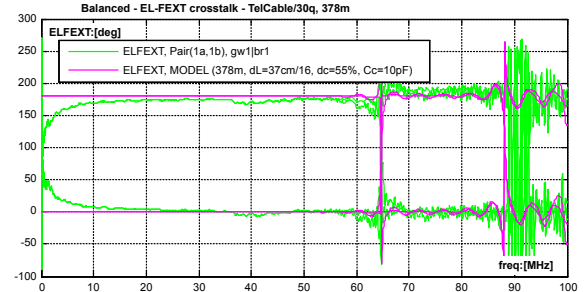


Fig. 8. Match of EL-FEXT phase, between model and measurement.

### 4.2 Impact of steps per twist

To verify if the number  $n$  of homogeneous sections per twist is large enough, we simulated the same cable length several times with an increasing number  $n$ . Figure 9 shows the simulated transfer and FEXT crosstalk of a 378m loop when we evaluate it for  $n=4, 16$  and 64 sections per twist respectively. This figure illustrates that this number hardly influences the result and that even a simulation with just 4 section per twist is adequate.

## 5 SENSITIVITY TO GEOMETRIC VARIATION

Now the model has proven to be reliable, we can use it to analyze the impact of changing some design parameters of the cable. This includes the impact of designing a cable with a tighter/looser twist or smaller/bigger variations of wire capacity to shield, or the impact of that nominal capacitance.

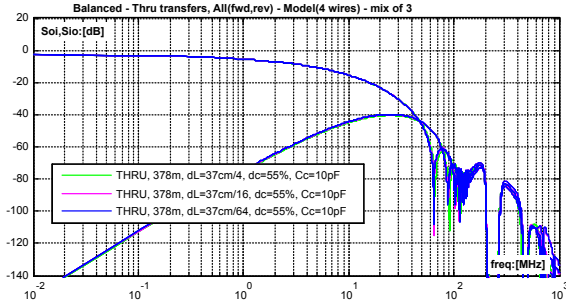


Fig. 9. A simulation with only 4 steps per twist offers similar result as a simulation with 64 steps per twist.

**5.1 Sensitivity to twist length  $\Delta L$**

Figure 10 shows the simulated results on the same loop when the twist length  $\Delta L$  varies from 3 to 300 cm. It shows three curves, each of them representing EL-FEXT (ratio between FEXT and direct transmission) at another twist length (distance of a full 360° turn of a quad). All other parameters are assumed to be at the nominal values of table 1 and 2, so the quad is assumed to be perfectly symmetrical causing the first order slope (20 dB/decade) to be absent.

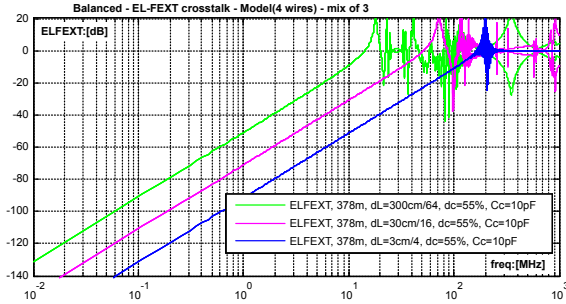


Fig. 10. An increase of twist-length by a factor 10 increases the EL-FEXT by 20 dB.

A first observation is that the slope of the second order EL-FEXT is accurately 40 dB/dec over a very wide frequency interval. Another observation is that when the twist becomes tighter, the magnitude of this second order effect drops. A decrease of twist length by a factor 10 results in 20 dB reduction of EL-FEXT. In other words: the EL-FEXT is proportional to the twist length in this region. In addition, when the second-order EL-FEXT approaches the value one, the "meandering" around that asymptotic value becomes seemingly random in appearance, since it quite in this region sensitive to small changes in assumptions.

**5.2 Sensitivity to shield unbalance  $\Delta C$**

Figure 11 shows various EL-FEXT curves for the same loop length when the variation between minimum and maximum capacitance from wire to shield changes. It shows five curves where the shield unbalance  $\Delta_c$  (as defined in table 2) varies in steps from 1% to 80%. This shield unbalance appeared to have a significant impact on the second order EL-FEXT. Each increase by a factor 10 causes 40 dB increase in EL-FEXT. But in all cases the slope of the second order

EL-FEXT remains accurately 40 dB/decade over a very wide frequency interval.

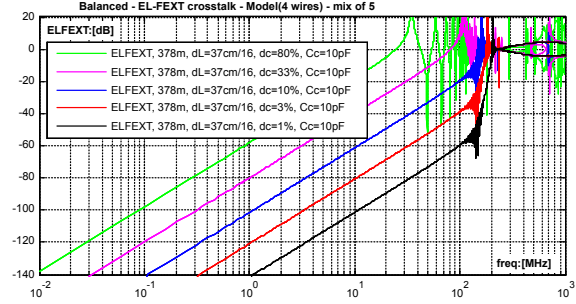


Fig. 11. An increase of the unbalance in capacity to shield by a factor 10 increase the EL-FEXT by 40 dB.

**5.3 Sensitivity to capacitance to shield**

The nominal capacitance between wire and shield is not only determined by the nominal distance but also by the wire gauge and the dielectric in-between. Figure 12 shows four curves of EL-FEXT, where the (nominal) capacity  $C_c$  varies from 0.1 pF to 100 pF. And all other parameters remain as defined in table 1 and 2. This time, the EL-FEXT does not change linearly with this capacity. In our example, it changes about 20 dB from 0.1 to 1 pF, 18 dB from 1 to 10 pF and about 9 dB from 10 to 100 pF.

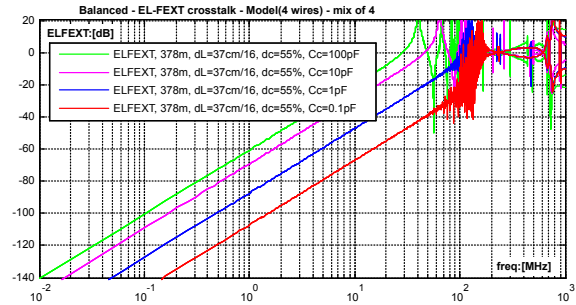


Fig. 12. An increase of the nominal capacitance between wire and shield increase the EL-FEXT in a non-linear way.

**6 LENGTH-DEPENDENCY OF FEXT**

The overall EL-FEXT increases with the cable length and is a combination of both the first and the second order behavior of the EL-FEXT. Both have a different origin and there is no reason why both should scale equally with the cable length.

The origin of the first order crosstalk effect is well known and originates from random perturbations of the geometry [10], [11]. When the four wire are positioned in a perfect square, and this symmetry would not have been disturbed by a shield, then there will be no crosstalk. But in practice this perfection is easily disturbed by random variation of the position and size of each wire. This causes crosstalk. Moreover, it is also well known that the associated EL-FEXT scales with the root of the cable length (in a statistical sense) and with a slope of 20 dB/decade [10], [11].

The second order effect even occurs in the full absence of these random perturbations, and even when the wires are positioned in a perfect square. The presence of a shield can disturb the electrical balance between opposite wires and the presence of twisting can reduce this effect significantly but not completely. This all makes the second order effect more deterministic in nature, and makes it plausible that it increases proportionally with the cable length.

In practice, however, there will always be a combination of both the first and the second order effect, and both will scale differently with the cable length. To prove the statements of the previous section, we will make our model more realistic and cover both the first and the second order effect in the same simulation. We have added random variation of capacitances around their nominal values, and apply these random changes to each small (uniform) section of the cascade calculation. This required a brute force cascade calculation of a huge number of uniform sections, where the capacitors  $C_p$  and  $C_q$  are randomly "jittered" for about 1% around their deterministic values table 1. This causes a first order behavior of the EL-FEXT, in superposition with the second order behavior.

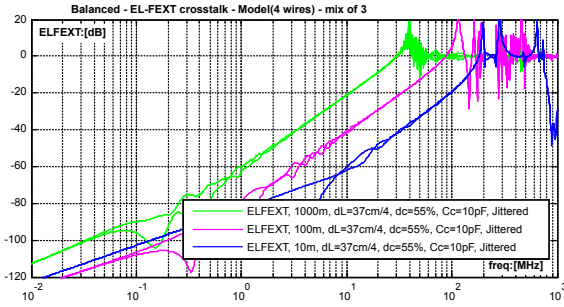


Fig. 13. Simulated EL-FEXT magnitude as function of the loop length.

Figure 13 shows three EL-FEXT curves from these brute force simulations, where the loop length varies in steps from 10 m via 100 m to 1000 m. The low frequency part of these curves (below about 1 MHz) show that the first order EL-FEXT increases a bit random with the loop length. Roughly 10 dB when the length increase by a factor 10. This demonstrates that the first order EL-FEXT increase roughly proportionally with the square root of the cable length, but this increase holds only in a statistical sense (averaged over many of these experiments). The mid band frequencies of these curves (between about 1 and 100 MHz) show that the second order EL-FEXT increases consistently by 20 dB when the length increases by a factor 10. This demonstrates the expected linear increase of the EL-FEXT with the loop length. At higher frequencies, all EL-FEXT curves meander almost randomly around the value of 0 dB.

Figure 14 shows two groups of curves, representing the phase of the two forward EL-FEXT curves in the same quad. In all cases they have roughly opposite values around 0 and 180 degrees over the frequency band where the second order effect dominates.

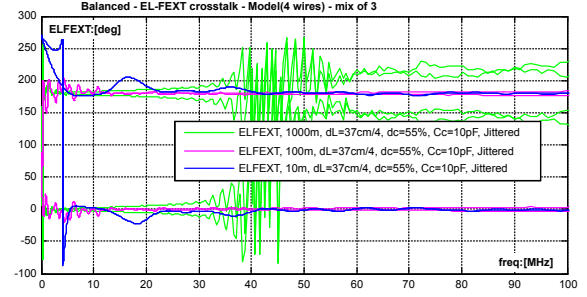


Fig. 14. Simulated EL-FEXT phase as function of the loop length; they have opposite values in the same direction.

## 7 SIMPLIFIED EL-FEXT MODEL

For system performance calculations on DSL systems, the brute force approach of our model is a bit overkill. Therefore a simplified approximate model of EL-FEXT as function of the frequency and of the cable may be preferred in these cases. This means the use of a simple transfer function  $H_{ELFEXT}(j\omega, L)$ , to approximate the magnitude of the EL-FEXT as function of frequency and cable length  $L$ .

The legacy model [10], [11] using that approach is a first order transfer function and is too simple for higher frequencies. The model in [21]:sect A.2.3.1 with just two straight lines is also too simple since it ignores that those two lines scale differently with the cable length. It also ignores that the EL-FEXT cannot keep growing to infinite high values for increasing frequencies. Therefore we refined the approach being suggested before in [5] which is based on a transfer function description of second order high-pass filters in general.

The second order transfer function in equation 6 can model the magnitude of EL-FEXT curves much better, since it (a) supports both the first and second order slope, has (b) an asymptotic limitation for higher frequencies at 0 dB, scales (c) the first order slope with the root of the cable length and scales (d) the second order slope linearly with the cable length. The transfer function is defined in such a manner that the overshoot near 0 dB is insignificant.

$$H_{ELFEXT}(j\omega, L) = \left\| \frac{k_1(L) \cdot \left(\frac{j\omega}{\omega_0}\right) + k_2(L) \cdot \left(\frac{j\omega}{\omega_0}\right)^2}{1 + (k_1(L) + \sqrt{k_2(L)}) \cdot \left(\frac{j\omega}{\omega_0}\right) + k_2(L) \cdot \left(\frac{j\omega}{\omega_0}\right)^2} \right\| \quad (6)$$

$$\text{where } k_1(L) = K_{XF1} \cdot \sqrt{L/L_0}, \text{ and } k_2(L) = K_{XF2} \cdot (L/L_0)$$

In this expression,  $\omega_0$  and  $L_0$  are arbitrary scaling constants (e.g. 1 MHz and 1 km), and  $K_{XF1}$  and  $K_{XF2}$  are empirical values for matching the EL-FEXT characteristics between particular wire pairs of interest. To model our example cable, values like  $K_{XF1} = -68.2$  dB and  $K_{XF2} = -76.6$  dB, both normalized to 1 MHz and 1 km cable, are adequate. When  $K_{XF2} = 0$  this enhanced model approximates the legacy model for EL-FEXT, since  $K_{XF1}$  is usually  $\ll 1$ .

Figure 15 and 16 illustrate how the formula of the simplified EL-FEXT model behaves for different loop lengths. The red lines, specified by  $k_1 \cdot (\omega/\omega_0)$  and  $k_2 \cdot (\omega/\omega_0)^2$ , are the asymptotes of these blue curves. The asymptote raising

with 20 dB/decade scales proportionally with the root of the loop length  $L$ , since  $k_1(L) = K_{XF1} \cdot \sqrt{L/L_0}$ . The asymptote raising with 40 dB/decade respectively, scales proportional with the loop length  $L$ , since  $k_2(L) = K_{XF2} \cdot (L/L_0)$ . They cross each other near 3.3 MHz for the 1000 m loop and near 10 MHz for the 100 m loop. The blue line is limited near 0 dB so the blue curve has the desired behavior over the full frequency band. When adequate values for  $K_{XF1}$  and  $K_{XF2}$  are found to match a particular cable of interest, the simplified model offers a fair description of the EL-FEXT over a wide range of frequencies and loop lengths.

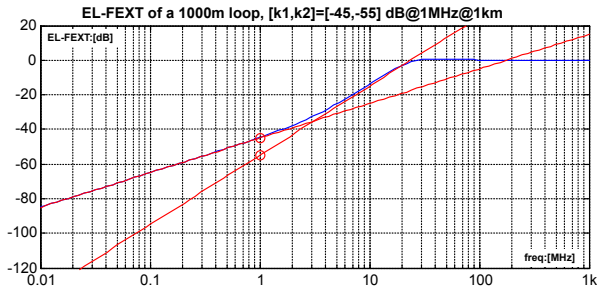


Fig. 15. Result from simplified EL-FEXT model for a 1000 m loop and for  $K_{XF1} = -45$  dB and  $K_{XF2} = -55$  dB. The blue curve is the model, the red lines are its asymptotes  $k_1 \cdot (\omega/\omega_0)$  and are crossing each other near 3.3 MHz. The markers at 1 MHz through these asymptotes are representing the values  $K_{XF2}$  and  $K_{XF1}$ .

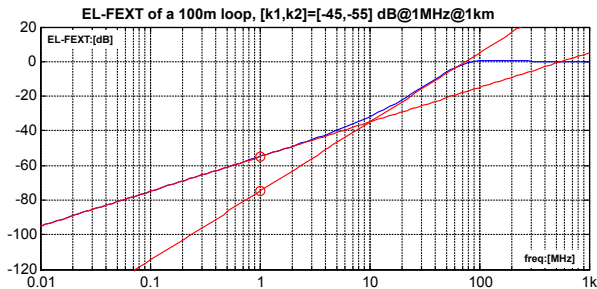


Fig. 16. Result from simplified EL-FEXT model for a 100 m loop and for  $K_{XF1} = -45$  dB and  $K_{XF2} = -55$  dB. The blue curve is the model, the red lines are its asymptotes  $k_1 \cdot (\omega/\omega_0)$  and  $k_2 \cdot (\omega/\omega_0)^2$ , and are crossing each other near 10 MHz.

## 8 CONCLUSIONS

It is well-known that the ratio between received crosstalk and received signal level in telephony cabling increases with the frequency, but the awareness that the increase of the in-quad EL-FEXT becomes much stronger above a certain frequency (40 dB instead of 20 dB per decade) was raised only recently [5], [12]. This increase puts strong demands on vectoring engines of DSL modems to let VDSL and G.fast make efficient use of higher frequencies. We elaborated on a full-8-port model of four wires in a quad, to quantify various characteristics of this dual slope behavior of in-quad EL-FEXT in these cables.

This model demonstrates that the first order and second order effects in in-quad EL-FEXT scale differently with the cable length. The well-known first order effect has random

perturbation of the geometry as origin, scales proportionally with the root of the cable length (in a statistical sense) and offers the EL-FEXT its slope of 20 dB/decade.

The second order effect is deterministic in nature. It occurs when the metallic surroundings of two wire pairs in a quad (e.g. a shield) disturb the balance of a perfect quad structure. Twisting the quad can reduce this effect significantly but a residue will always remain. This residue contributes a slope of 40 dB/decade to the in-quad EL-FEXT, and can dominate the first order effect above a certain frequency. It proceeds until the in-quad EL-FEXT approaches 0 dB. The magnitude will then meander with rapid variations around 0 dB.

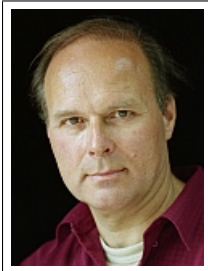
Our model also quantifies how this second order effect scales with various design parameters of the cable. It shows that (a) an increase of twist length by a factor 10 will increase this effect by 20 dB, (b) an increase of shield unbalance by a factor 10 will increase it by 40 dB, and (c) an increase of the average capacitance to shield will also increase it significantly but that effect is not linear.

The improved understanding of this second order crosstalk effect brought us to propose a simplified but adequate model of in-quad EL-FEXT [10], [11] for supporting system calculations on the performance of DSL systems. This takes more aspects into account than the simple model with two-lines described in [21].

## REFERENCES

- [1] P. Odling, T. Magesacher, S. Host, P. Borjesson, M. Berg, and E. Areizaga, "The fourth generation broadband concept," *IEEE Communications Magazine*, vol. 47, no. 1, pp. 62–69, 2009.
- [2] *Self-FEXT cancellation (vectoring) for use with VDSL2 transceivers*, ITU-T Std. G.993.5, 2015.
- [3] *Fast access to subscriber terminals (FAST) - Power spectral density specification*, ITU-T Std. G.9700, 2014.
- [4] *Very high speed digital subscriber line transceivers 2 (VDSL2)*, ITU-T Std. G.993.2, 2015.
- [5] R. v. d. Brink, "Dual slope behaviour of el-fext," TNO Contribution 2012-02-4A-038 to ITU-T SG15/Q4, Feb 2012.
- [6] R. v. d. Brink, Boschma, and Popova, "Wideband transfer and crosstalk measurements on twisted pair cables," TNO Contribution 11BM-021 to ITU-T SG15/Q4, Apr 2011.
- [7] R. v. d. Brink, "Wideband modelling of twisted pair cables as two-ports," TNO Contribution 11GS3-028 to ITU-T SG15/Q4, Sept 2011.
- [8] Magesacher, "Mtl - a multi-wire transmission line modelling toolbox," *Journal of Computer and Electrical Engineering*, vol. 5, no. 1, pp. 52–55, Feb 2013.
- [9] D. Acatauassu, S. Host, C. Lu, M. Berg, A. Klautau, and P. Borjesson, "Simple and causal copper cable model suitable for g.fast frequencies," *IEEE Transactions on Communications*, vol. 62, no. 11, pp. 4040–4051, 2014.
- [10] *Spectral management on metallic access networks; Part 2: Technical methods for performance evaluations*, ETSI Std. TR 101 830-2, Rev. V1.2.1, 2008.
- [11] *Transmission systems for communications*. Bell Telephone Labs, 1971, 4th edition.
- [12] R. v. d. Brink, "Far-end crosstalk in twisted pair cabling; measurements and modeling," TNO Contribution 11RV-022 to ITU-T SG15/Q4, Nov 2011.
- [13] Eriksson, Berg, and Lu, "Equal length fext measurements on pe05 cable," Ericsson Contribution 11RV-054R1 to ITU-T SG15/Q4, Richmond, Nov 2011.
- [14] "Equal-length fext measurements on pe05 cable," Huawei Contribution COM 15 - C 1864 to ITU-T SG15/Q4, Nov 2011.
- [15] Bruyssel and Maes, "Dual slope behaviour of el-fext," ALU Contribution 2012-06-4A-033 to ITU-T SG15/Q4, May 2012.
- [16] Humphrey, "On dual slope fext observations," BT Contribution 2012-05-4A-021 to ITU-T SG15/Q4, May 2012.

- [17] Humphrey and Morsman, "Fext cable measurements," BT Contribution 2012-05-4A-025 to ITU-T SG15/Q4, May 2012.
- [18] Muggenthaler and Tudziars, "El-fext analysis," DT Contribution 2012-06-4A-041 to ITU-T SG15/Q4, May 2012.
- [19] Bongard, "Dual slope elfext behaviour on swiss cables," Swisscom contribution 2013-01-Q4-042 to ITU-T SG15/Q4, Feb 2013.
- [20] Schneider, Kerpez, Starr, and Sorbara, "Transfer functions, input impedance and noise models for the loop end," Cosigned contribution bbf2014.066 to Broadband Forum, March 2014.
- [21] *Broadband Copper Cable Models, Issue 1*, Broadband Forum Std. TR-285, Feb 2015.
- [22] *Broadband Copper Cable Models, Issue 1 corrigendum 1*, Broadband Forum Std. TR-285, Nov 2015.
- [23] Kozarev, Strobel, Leimer, and Muggenthaler, "Modeling of twisted-pair quad cables for mimo applications," Lantiq/DT Contribution bbf2014.467 to Broadband Forum, June 2014, (updated from bbf2014.377 and bbf2014.117).
- [24] U. Strobel, Stolle, "Wideband modeling of twisted-pair cables for mimo applications," *Globecom 2013 - Symposium on Selected Areas in Communications*, pp. 2828–2833, Dec 2013.
- [25] R. v. d. Brink, "Understanding and modelling the dual slope effect on el-fext," TNO Contribution 2016-04-Q4-021 to ITU-T SG15/Q4, April 2016.
- [26] —, "Enabling 4gbb via hybrid-ftth, the missing link in ftth scenarios," TNO Contribution bbf2010.1395 to Broadband Forum, Dec 2010.
- [27] C. Paul, *Analysis of Multiconductor Transmission Lines*. Wiley-IEEE Press, 2008.



**Rob F.M. van den Brink** graduated in Electronics from Delft University in 1984, and received his PhD in 1994. He works as a senior scientist within TNO on broadband access networks. Since 1996, he has played a very prominent role in DSL standardization in Europe (ETSI, FSAN), has written more than 100 technical contributions to ETSI, and took the lead within ETSI-TM6 in identifying / defining cable models, test loops, noise models, performance tests, and spectral management. He is the editor of an ETSI-TM6

reference document on European cables, and led the creation of the MUSE Test Suite, a comprehensive document for analyzing access networks as a whole. He also designed solutions for Spectral Management policies in the Netherlands, and created various DSL tools for performance simulation (SPOCS, [www.spocs.nl/en](http://www.spocs.nl/en)) and testing that are currently in the market. He has been Rapporteur/Editor for ETSI since 1999 (on Spectral Management: TR 101 830), Board Member of the MUSE consortium (2004-2008, [www.ist-muse.org](http://www.ist-muse.org)) and is now (since 2009) Work Package leader of various projects of the Celtic 4Gbb Consortium (2009-2017, [www.4gbb.eu](http://www.4gbb.eu)). This consortium was multiple awarded for initiation the development and standardization of G.fast.